PROGRESS IN PHOTOVOLTAICS: RESEARCH AND APPLICATIONS, VOL 1, 255–267 (1993)

Research

Metastability of Phosphorus and Boron in Hydrogenated Amorphous Silicon

C. E. Nebel[1], R. A. Street[2], N. M. Johnson[2] and W. B. Jackson[2]

[1]*Institut für Physikalische Elektronik, Universität Stuttgart, 70569 Stuttgart 80, Germany;* [2]*Xerox Palo Alto Research Center, Palo Alto, CA 94304, USA*

Thermodynamic equilibration kinetics of phosphorus- and boron-doped hydrogenated amorphous silicon (a-Si:H) are explored using dark conductivity measurements. The equilibration kinetics of phorphorus- and boron-doped a-Si:H are different and there is a strong dependence on the deposition temperature (T_s). Small variations in temperature of the semiconductor cause variations in active dopant concentration, which affects the conductivity. The transformation of phorphorus into the electronically active phase (activation) follows a stretched exponential time dependence with a temperature-independent dispersion parameter, β, of 0.85, whereas the transformation into the electronically passive bonding configuration (passivation) is also a stretched exponential but with $\beta \leqslant 0.8$. The kinetics of boron metastability are similarly a stretched exponential, but with equal β values for activation and passivation. The time constant, τ, to achieve equilibrium for both transformations is thermally activated with energies $E_{act} \approx 1.1$ eV for phosphorus and boron. An increase in T_s leads to an increase of E_{act}. The data are discussed and interpreted based on the hydrogen migration model.

INTRODUCTION

The application of amorphous hydrogenated silicon (a-Si:H) in solar cells was initiated by the discovery that the electronic properties of a-Si:H can be controlled over a wide range by adding phosphine or diborane to the silane gas during the film growth.[1,2] By varying the gas ratio, the Fermi level can be shifted in the gap between the conduction band and the valence band (mobility gap) over 1.2 eV. In combination with the excellent photoconductivity properties of a-Si:H, this discovery opened the way for a large number of device applications, of which one of the most important and promising is the p-i-n solar cell. It turned out, however, that doping of a-Si:H is a very complex phenomenon, which up to now has only been partially understood. It is well documented that substitutional doping is accompanied by an increase in defect density,[3,4] which has been explained successfully by Street's defect compensation model.[5] Recently it has been demonstrated that the density of localized states in a-Si:H is only partially defined during film growth but is controlled also by a glass-like thermal equilibrium that exists above a certain glass-transition temperature T_E.[6,7] This equilibrium is established by the motion of hydrogen.[8] When a sample is cooled to temperatures below T_E, the atomic and electronic structure is frozen in. The electronic properties at room temperature are

1062–7995/93/040255–13 $11.50

Received 20 March 1993
Revised 24 May 1993

therefore defined by the thermal equilibrium state at $T = T_E$. The dopant atom, being less constrained by the surrounding amorphous structure than by a crystalline network, is free to adopt either a coordination that is electronically active or inactive (see below). It has been shown that the doping efficiency, which is the ratio of active to passive dopant density, is also affected by the thermal history of the specimen[6,7] and the applied electric field.[9,10] Obviously, at temperatures $T > T_E$ an additional amount of passively built-in dopant is transferred into the active configuration.

Device applications are sensitively dependent on the doping efficiency, which affects the Fermi level and also therefore basic features such as contact properties, internal fields, photoconductivity, etc. In p-i-n solar cells, for example, the built-in field that governs the solar cell efficiency is sensitively dependent on the Fermi levels in the n and p layers. A decrease of the doping efficiency caused by thermal or by bias effects reduces the internal field, and vice versa. This paper elucidates effects that are related to thermally induced dopant metastability in a-Si:H. The understanding of dopant metastability and its dependence on the Fermi level and on hydrogen migration is a fundamental step towards further improvement of p-i-n a-Si:H solar cells.

Based on a variety of investigations the following characteristics of doping in a-Si:H have been discovered. Dopants are built into the growing amorphous structure in a preferentially threefold coordinated manner (P_3, B_3), resulting in an electronically inactive bonding configuration.[11,12] The thermodynamic equilibrium during the growth of the sample determines the fraction of fourfold coordinated, electronically active dopants (P_4, B_4), which is typically orders of magnitude smaller ($P_4/P_3 \leqslant 10^{-2}$) than the number of inactive dopants.[12] It is surprising that, despite this phenomenon, conductivity enhancements over several orders are achieved, accompanied by a shift of the Fermi level. Details investigations of the doping mechanism reveal significant differences compared to the well-understood doping of crystalline semiconductors. The fourfold coordinated dopant is stable only when ionized and an approximately equal density of charged dangling bonds (broken and doubly occupied Si bonds) are created.[11,12] The Fermi level lies approximately in the minimum between the charged defect distribution, to which we refer in the following as D^- in the case of phosphorus or D^+ in the case of boron doping, and the tail state distribution.[13,14] The doping level of the P_4 or B_4 states is masked by the much higher number of band tail states.[15] From charge neutrality conditions it is obvious that, for example, in the case of phosphorus doping[13]

$$P_4^+ = D^- + n_{BT} + P_4^0 \tag{1}$$

where n_{BT} is the fraction of electron density in the conduction band tail and P_4^0 is the density of occupied P_4 centres that can be detected by electron spin resonance experiments.[7,12] Sweep-out experiments have been applied to measure the band tail carrier density n_{BT}[10,15] and photothermal deflection spectroscopy (PDS)[13,16] or constant photocurrent experiments (CPM)[17] to determine the defect distribution. Doping of a-Si:H leads predominantly to an increase of charged defects and is well described by

$$P_4^+ \approx D^- \tag{2}$$

The band tail carrier density n_{BT} and P_4^0 are small quantities compared to the D^- and P_4^+ densities. Some of the large number of threefold coordinated impurities are transformed into the active configuration ('dopant activation') by increasing the temperature above T_E[7,15] or by applying a reverse bias field.[9,10] Decreasing the temperature T or the reverse bias voltage leads to the opposite effect, which we refer to as 'dopant passivation'. The 'hydrogen glass' model attributes the metastable changes to the hydrogen migration in the host lattice of the amorphous Si structure.[8,13,16,18] Above the 'freezing-in' temperature, T_E, which is about 130°C for phosphorus-doped and about 90°C for boron-doped a-Si:H, the structure is in thermodynamic equilibrium and everything below it is 'frozen-in'. The phrase 'frozen-in' describes the situation of a considerably slowed down relaxation process towards the thermodynamic equilibrium. The freezing-in temperature is Fermi level-dependent, increasing to higher temperatures with increasing activation energy of the conductivity.[17] This is in agreement with data determined for hydrogen diffusion, where the migration is fast in highly doped a-Si:H and slow in weakly doped and intrinsic material.[7,8,16] The relaxation of frozen-in band tail carriers has been investigated

by sweep-out experiments on P- and B-doped a-Si:H, which follows a stretched exponential time dependence[7,15,16]

$$\Delta n_{BT}(t) = \Delta n_{BT_0} \exp\left[-\left(\frac{t}{\tau}\right)^{\beta}\right] \tag{3}$$

where Δn_{BT} is the excess carrier density; τ is the relaxation time constant, which is thermally activated

$$\tau = \tau_0 \exp\left(\frac{E_{act}}{kT}\right) \tag{4}$$

E_{act} is typically in the range ≈ 1 eV, and $10^{-12}\,s^{-1} \leqslant \tau_0 \leqslant 10^{-10}\,s^{-1}$.[8,13,19] Both parameters have been reported to be doping level- and dopant-dependent;[19] β is the dispersion parameter, given by

$$\beta = \frac{T}{T_0} \tag{5}$$

where T_0 is ca. 600 K.[8,18] Up to now no significant changes in defect structure coinciding with dopant metastability have been detected.[13,16] From the charge neutrality conditions (Equation (1)) we conclude that the metastable variation in active dopants leads to an equal variation in band tail electron or hole concentration

$$\Delta P_4^+(t) \approx \Delta n_{BT}(t) \tag{6}$$

The relaxation of excess carrier density therefore follows the time-dependent variation of active dopants.

Data available in the literautre on dopant activation and passivation have been measured by sweep-out experiments.[10,15] This method is excellent to determine the band tail carrier density but requires a sophisticated sample structure. The dynamic range of the detection system is limited, which restricts the application to large signals, meaning large deviations from equilibrium. In this paper we introduce a novel method: we apply 'dark conductivity' experiments measured as a function of time after imposing a change in thermodynamic equilibrium. Although only carriers above the mobility edge are detected experimentally, the advantage is the high sensitivity range, which allows the investigation of even the smallest relaxations on homogeneously doped layers in a simple coplanar contact configuration. A discussion of this method will be given in the next section.

The investigation of dopant metastability elucidates the mechanisms of structural metastability in disordered semiconductors such as a-Si:H. Information about interactions of electrons and holes with defects and dopants and about hydrogen migration can be deduced. Interesting problems that can be resolved at least partially by these investigations are the involvement of hydrogen and its bonding configuration, migration and charge state.

We introduce experimental data measured on phosphorus- and boron-doped a-Si:H where the kinetics of the relaxation, its activation energy, the dispersion parameter and the dependence of the relaxation time constant on deviations from equilibrium are points of interest. Finally, we discuss and interpret the data and include a brief summary.

EXPERIMENTAL

When using DC dark conductivity experiments to monitor metastable variations of dopants we have to take into account the specific features of transport in a-Si:H. Only carriers above the mobility edge are mobile and the conductivity is commonly described by

$$\sigma = q\mu_c n_c \tag{7}$$

where n_c is the free carrier density above the mobility edge, μ_c is the free carrier mobility and q is the

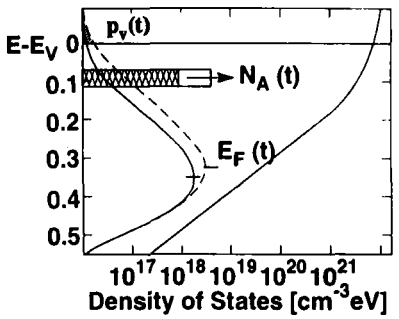

Figure 1. Variation of the hole distribution and density in the valence band tail due to the increase of the dopant density N_A by dopant activation. The free hole density $p_v(t)$ (see shaded regions) at $E \leqslant E_v$ increases proportionally to $N_A(t)$, which is shown in Figure 2

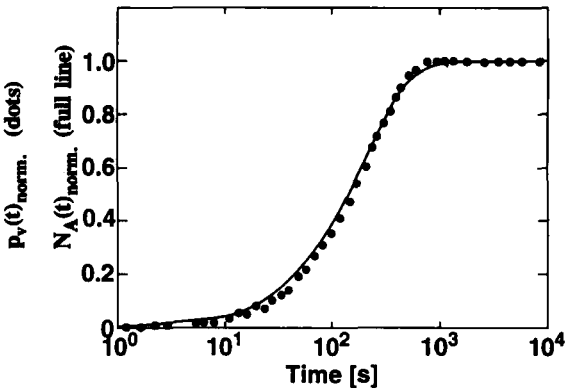

Figure 2. Normalized variation of the free hole density $p_v(t)$ (●) and dopant density $N_A(t)$ (———) calculated for the density of state distribution shown in Figure 1

elementary charge. We suppose that the free carrier mobility is not affected by a small variation in dopant density.

A critical point of discussion is whether the variation in active dopants is displayed accurately in the variation of the free carrier density. To discuss this problem we consider the case of holes, owing to the fact that the valence band tail is much broader than the conduction band tail, which causes deep trapping of holes with only a small fraction in the extended states of the band. Results deduced by these calculations are also valid for electrons or situations where carriers are distributed in comparable or steeper tails. In Ref. 15 a detailed discussion of the density of states (DOS) distribution as well as of carriers in doped a-Si:H has been given. Figure 1 displays schematically the valence band tail with an Urband energy of 50 meV. For the discussion of the free carrier density variation as a function of variation in dopant density we assume an exponential time-dependent variation of the dopant density N_A, given by

$$N_A(t) = N_{A0} + \Delta N_{A0}\left[1 - \exp\left(-\frac{t}{\tau}\right)\right] \tag{8}$$

where N_{A0} is the initial dopant density (acceptors), ΔN_{A0} is the variation of dopant density and τ is the time constant. We assume that the defect density is invariant. The increase in dopants results in an increase of holes, which leads to a redistribution in the tail and a shift of the Fermi level closer towards the mobility edge. The variation in hole density is given by

$$p_{tot}(t) = N_A(t)\left\{1 - \exp\left[-\frac{E_F(t) - E_A}{kT}\right]\right\} \tag{9}$$

where $E_F(t)$ is the Fermi energy and E_A is the energy level of the dopant; p_{tot} is also given by

$$p_{tot}(t) = \int_0^\infty g(E)[1 - f(E)]\,dE \tag{10}$$

where $g(E)$ is the DOS distribution and $f(E)$ the Fermi function. Finally, the hole density in the transport levels ('free hole density') is given by

$$p_v(t) \approx g(E_v)kT \exp\left[-\frac{E_F(t) - E_v}{kT}\right] \tag{11}$$

Table I. Data of the a-Si:H samples under investigation[a]

Doping level	Deposition temperature (°C)	Equilibrium temperature (°C)	E_{act} ($T < T_E$) (meV)	E_{act} ($T = T_E$) (meV)	E_{act} ($T > T_E$) (meV)
10^{-3} PH_3/SiH_4	200	115	286	270	190
10^{-3} PH_3/SiH_4	350	135	270	248	175
10^{-4} PH_3/SiH_4	250	121	278	340	160
10^{-2} B_2H_6/SiH_4	200	80	434	353	317
10^{-3} B_2H_6/SiH_4	200	92	453	398	360

[a] The samples have been prepared using a conventional RF glow discharge deposition. The activation energies E_{act} have been calculated from the slopes of the conductivities, plotted on a semi-logarithmic scale versus $1/T$ in the case of $T > T_E$ and $T < T_E$, whereas E_{act} at $T = T_E$ is determined by the use of conductivity pre-factor $\sigma_0 = 150\ S\ cm^{-1}$ (T_E is the freezing-in temperature of the structure, measured by quenching-in experiments).

where $g(E_v)$ is the DOS at the valence band mobility edge E_v. With the DOS shown in Figure 1 and the acceptor density variation described by Equation (8) we have calculated numerically the variation of the free hole density. Figure 2 shows the normalized time dependence of the dopant concentration (full line), which is reasonably well represented by the variation of the free hole density (dots). Even for tails with Urbach energies larger than 50 meV, we calculate a reasonable agreement between the time-dependent variation of the dopant and the carrier density. We conclude, therefore, that the application of DC dark conductivity to monitor the kinetics of metastable boron and phosphorus concentrations is justified and is a sensitive alternative to sweep-out experiments.

The experiments are performed on samples prepared at substrate temperatures, T_s, of 200 and 350°C with a gas phase ratio of 10^{-3} PH_3/SiH_4, and at $T_s = 230$°C with a gas phase ratio of 10^{-4} PH_3/SiH_4 in a conventional RF glow discharge reactor. The boron-doped a-Si:H has been deposited in the same reactor at $T_s = 200$°C where the gas phase ratio has been varied between 10^{-3} and 10^{-2} B_2H_6/SiH_4. A summary of the specimens is given in Table I.

Chromium contacts have been evaporated in coplanar contact configuration on to the samples. Ohmic characteristics are achieved by introducing 40-nm thick highly doped layers between the Cr contacts and a-Si:H. To determine the freezing-in temperature, T_E, the doped a-Si:H samples were heated to 180°C, followed by rapid cooling in H_2O; T_E is slightly dependent on doping level. More significant, however, is the deposition temperature (T_s) dependence, which raises T_E from about 120 to 135°C when T_s is increased from 200 to 350°C (see Table I).

In order to measure temperature-induced equilibration kinetics, abrupt temperature variations have been realized by transferring the sample into an oil bath of higher (increase of dopant density: 'activation') or lower (decrease of dopant density: 'passivation') temperature than the temperature at which the sample has been annealed for up to 48 h. After the very fast (<2 s) establishment of the new temperature, T_M, the conductivity was monitored as a function of time. Figure 3 shows typical time-dependent variations recorded on phosphorus-doped a-Si:H after fast cooling from $T_A = 435$ K to $T_A = 388$ K and after a fast temperature increase from $T_A = 350$ to $T_M = 388$ K. In all the evaluated cases the measurement temperature, T_M, was established within times of less than 2 s. The oil is highly resistive, with no detectable effects on the conductivity. Comparisons of sample properties before and after the oil treatments revealed no irreversible changes. The variations in conductivity during the approach to the new thermodynamic equilibrium were typically in the range 5–30%. The deduced data therefore represent small perturbations from equilibrium.

In the following we show transient currents normalized by

$$I(t)_{norm.} = \frac{I(t) - I(t \to \infty)}{I(t = 0) - I(t \to \infty)} \tag{12}$$

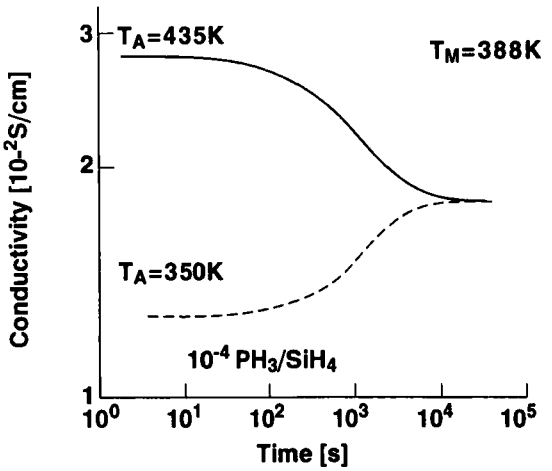

Figure 3. Typical transient conductivities of phosphorus-doped a-Si:H, where T_M is the temperature at which the conductivities have been recorded and T_A the temperatures at which the sample have been kept prior to T_M: (———) phosphorus passivation; (– – – –) activation

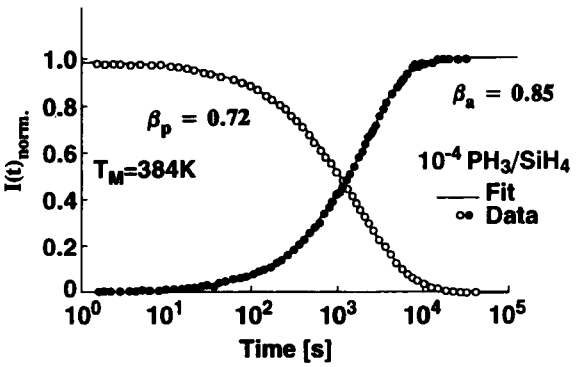

Figure 4. Normalized transient currents measured on phosphorus-doped a-Si:H at $T_M = 384$ K. Although both activation (●) and passivation (○) kinetics are stretched exponentials, the dispersion parameter of the passivation, β_p, is 0.72 whereas the activation is well described by $\beta_a = 0.85$

for the case of dopant passivation, and by

$$I(t)_{\text{norm.}} = \frac{I(t) - I(t=0)}{I(t \to \infty) - I(t=0)} \tag{13}$$

for the case of dopant activation, where $I(t = 0)$ is the current at the beginning of the experiment, $I(t \to \infty)$ is the current of the equilibrated state and $I(t)$ is the time-dependent variation of the current recorded by computerized apparatus.

METASTABILITY OF BORON- AND PHOSPHORUS-DOPED a-Si:H

Figure 4 shows normalized (dots) current transients with least-square fits (full lines) to the data calculated based on Equation (3). The relaxation towards the new equilibrium of the 10^{-4} PH_3/SiH_4-doped a-Si:H after rapid cooling as well as after fast heating follows stretched exponential kinetics but with significantly different dispersion parameters. The passivation at $T_M = 384$ K is well described over the entire time regime by a stretched exponential time dependence with $\beta_p = 0.72$, whereas the activation at the same temperature takes place with $\beta_a \approx 0.85$. Figure 5 shows the passivation of excess dopants and Figure 6 the activation, measured at different temperatures. The passivation obeys a temperature dependence with β_p increasing from 0.65 at $T_M = 384$ K to 0.77 at $T_M = 441$ K. The stretched exponential activation is temperature independent with $\beta_a \approx 0.85$. This result is summarized in Figure 7 together with data deduced on a 10^{-3} PH_3/SiH_4-doped layer. Applying Equation (5) results in a T_0 value of 575 K, which is in reasonable agreement with the value of 600 K determined by sweep-out experiments.[8] A difference between activation and passivation kinetics of phosphorus-doped a-Si:H was also found by Liu and Spear,[10] although they deduce $\beta_a = 1$. We attribute the discrepancy in β_a to the fact that Liu and Spear measured the activation after a reverse bias annealing, which causes strong deviations from the equilibrium, whereas our data are related to small perturbations. It has been shown in Ref. 13 that relaxation dynamics are sensitively dependent on the amplitude of perturbation of the equilibrium.

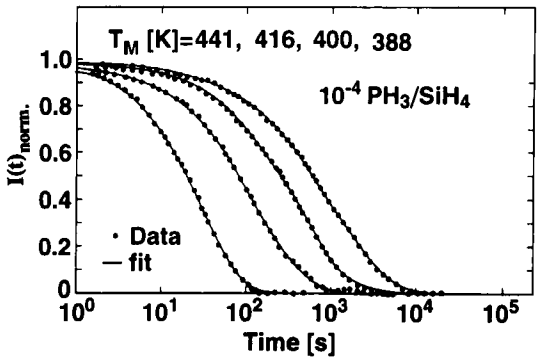

Figure 5. Normalized currents (●) representing phosphorus passivation measured at different temperatures. Also shown are the least-squares fits (———)

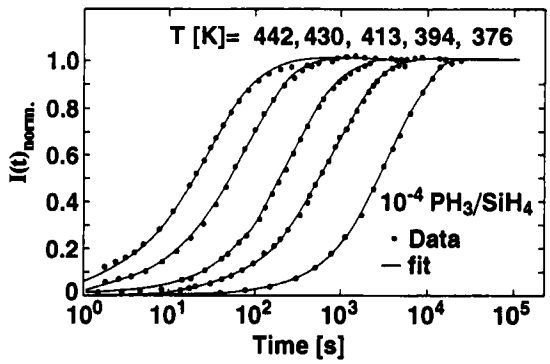

Figure 6. Transient currents (●) measured on phosphorus-doped a-Si:H at various temperatures, representing the creation of additional active phosphorus. Also shown are the calculated least-squares fits (———)

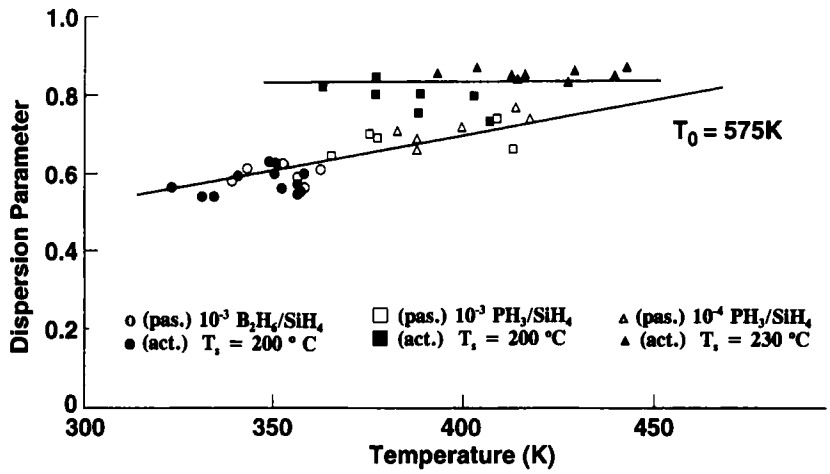

Figure 7. Temperature dependence of the dispersion parameter. Phosphorus-doped a-Si:H shows a strong asymmetry in passivation and activation kinetics whereas boron-doped a-Si:H is symmetric

Figure 8 shows transient features of a 10^{-3} B_2H_6/SiH_4-doped a-Si:H layer. The activation and passivation are well described by stretched exponentials. The dispersion parameter, β, is slightly temperature dependent, as plotted in Figure 7, and lies in the range ≈ 0.6, which fits remarkably well with the overall temperature dependence deduced from passivation experiments on phosphorus-doped a-Si:H; β is not dependent on the amplitude of perturbation. Even very small deviations from equilibrium are annealed-out with a stretched exponential time dependence. Measurements on a 10^{-2} B_2H_6/SiH_4-doped sample lead qualitatively to the same result.

A comparison of data deduced on samples that have been prepared at significantly different temperatures reveals distinct differences. Figure 9 combines β data measured on 10^{-3} PH_3/SiH_4-doped a-Si:H layers prepared at T_s = 200 and 350°C. The data indicate an increase in dispersion towards higher substrate temperatures.

In Figure 10 the equilibration time constants, τ, of the activation and passivation experiments are shown. The equilibration is strongly dependent on doping level and dopant. With increasing doping, τ decreases. The boron metastable changes are about three orders of magnitude faster than those of phosphorus. The activation energies are in the range ≈ 1.1 eV for both boron and phosphorus and are

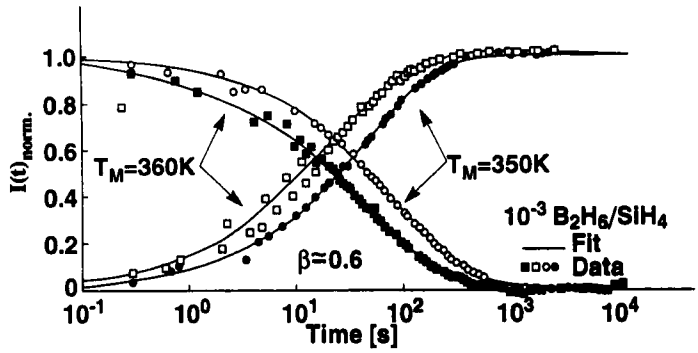

Figure 8. Normalized transient currents measured at T_M = 350 K and 360 K on boron-doped a-Si:H for the case of dopant activation (□, ●) and passivation (■, ○). Also shown are the least-squares fits (———)

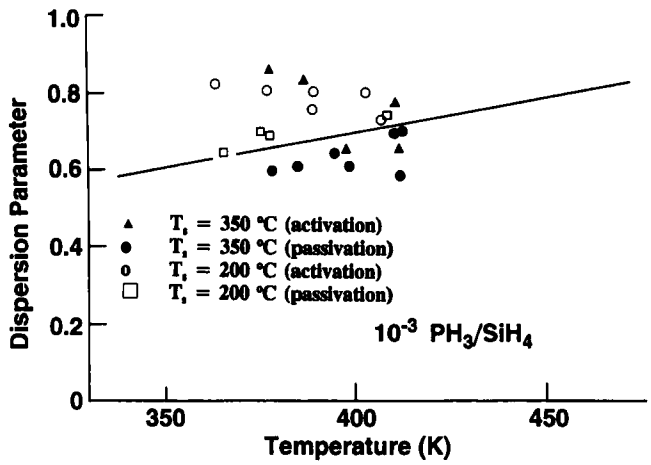

Figure 9. The effect of the deposition temperature, T_s, on the dispersion parameter, β. For comparison we have kept the doping ratio PH_3/SiH_4 constant at 10^{-3}, whereas T_s has been varied from 200°C to 350°C

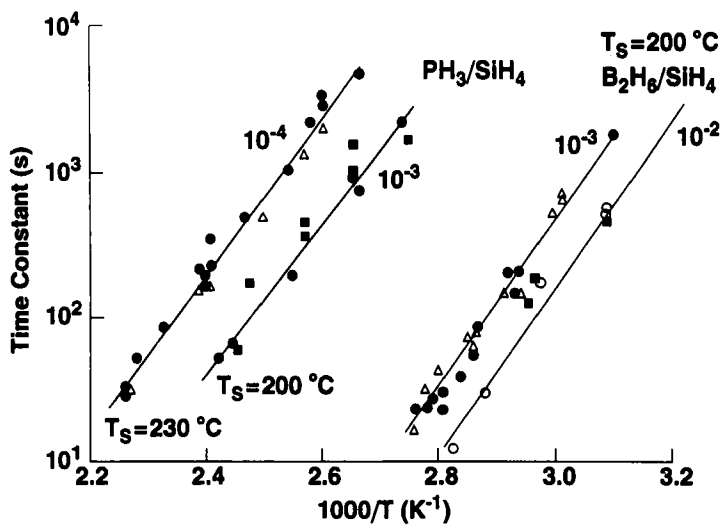

Figure 10. Time constants, τ, of the activation (△, ■) and passivation (○, ●) of phorphorus and boron

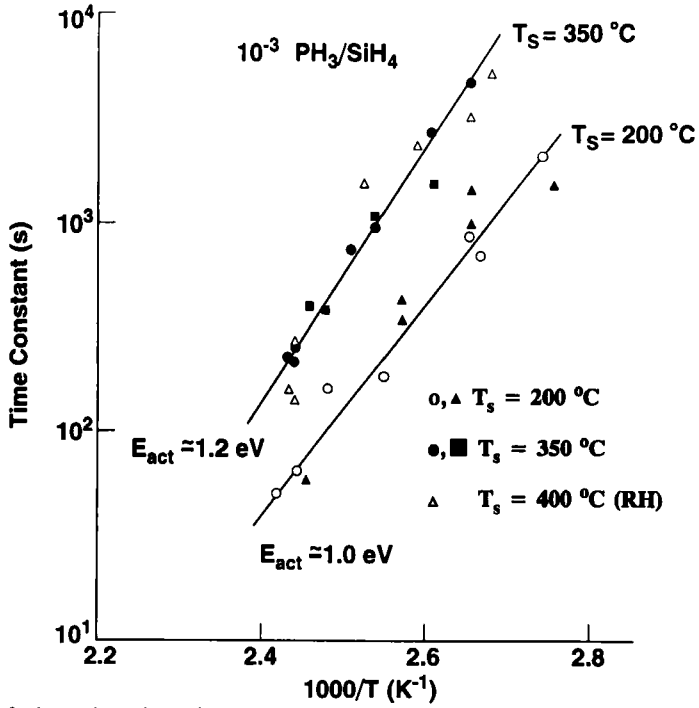

Figure 11. Comparison of the relaxation time constants measured on phosphorus-doped a-Si:H prepared at T_s = 200°C and 350°C (▲, ■: passivation; ○, ●: activation). Also shown are the data measured on a sample deposited at 400÷fi'C by a remote hydrogen (RH) plasma (△: passivation)

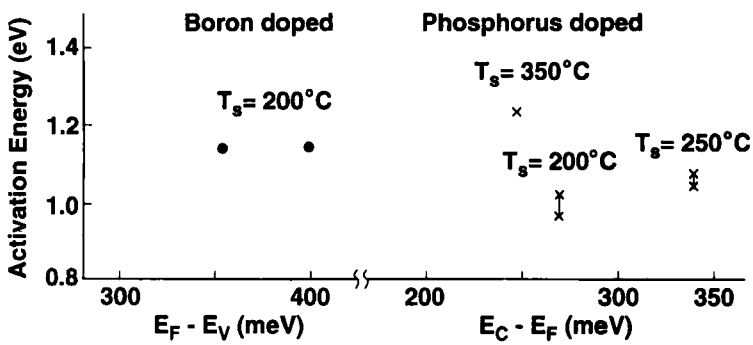

Figure 12. Activation energies of dopant activation/passivation dynamics plotted as a function of the Fermi level

not significantly dependent on the doping level or dopant. The variation of the deposition temperature affects the relaxation time constant and the activation energy; E_{act} increases from about 1.0 eV (T_s = 200°C) to 1.23 eV (T_s = 350°C), as displayed in Figure 11. We also show data deduced on a sample that has been deposited by a remote hydrogen plasma at T_s = 400°C.[20] Although the deposition process is very different compared to the conventional RF glow discharge technique, the data are comparable to the data deduced on a sample that has been prepared at T_s = 350°C in a conventional RF glow discharge. Figure 12 displays the activation energies versus Fermi level. Within the range of doping levels investigated, E_{act} is weakly dependent on the Fermi level. A significant deposition temperature dependence is, however, obvious.

DISCUSSION AND CONCLUSIONS

The data presented confirm results of previous measurements of phosphorus and boron passivation. It is demonstrated that structural relaxation is governed by a stretched exponential time dependence with interesting differences between phosphorus- and boron-doped a-Si:H. The measurements reveal different values of β for activation and passivation in n-type samples, while p-type a-Si:H has the same values. The relaxation kinetic is two orders of magnitude faster in boron-doped a-Si:H, although the activation energies of the equilibrations are comparable between phosphorus- and boron-doped a-Si:H. We find a significant influence of the deposition temperature on τ and E_{act}. The effect of the Fermi level in the relaxation kinetics on τ is obvious (see Figure 10 and Table I), while no significant influence on E_{act} can be detected. The underlying thermodynamics are well understood, but the analysis is very complicated when the DOS distribution for amorphous semiconductors is included. The equilibration process contains aspects related to the electronic states and aspects related to the atomic structure. The electronic states enter because the formation energies of dopants (and the related dangling bond defects) depend on the position of the Fermi energy, and the formation energies determine the equilibrium concentrations. There is a great amount of evidence that equilibration and metastability are mediated by hydrogen motion. A detailed discussion of hydrogen migration and the interaction with dopants can be found in Refs. 8, 19 and 21–24. The model has added complexity because the hydrogen motion itself depends on the electronic state. Thus, doping increases hydrogen diffusion, particularly in p-type material, and this is the underlying reason why the equilibration kinetics are faster in p-type material than in n-type material. It seems clear that the stretched exponential relaxation derives from the hydrogen bonding disorder.

The migration of hydrogen occurs by thermal excitation of deep hydrogen to shallow interstitial sites where hydrogen is mobile (see Figure 13). The equilibrium distribution of hydrogen is described by a hydrogen density of states (HDOS) and a Fermi function determined by the hydrogen chemical potential, μ_H. There is little experimental information about the shape of the HDOS or the detailed properties of the mobile hydrogen. The stretched exponential relaxation towards equilibrium indicates extensive disorder in the energies of both trapped and mobile hydrogen.

Taraskin[25] has pointed out that the time to achieve thermodynamic equilibrium is essentially the time until the levels at the hydrogen chemical potential, μ_H, are equilibrated. A well-established description of this process is the demarcation energy model. Here it is assumed that at time t, states at the demarcation energy E_D are just starting to re-emit hydrogen. This is described mathematically by

$$\nu(E)t = 1 \tag{14}$$

where ν is the re-emission frequency. The energy-dependent re-emission frequency is given by

$$\nu(E) = \nu_0 \exp\left(-\frac{E_I - E}{kT}\right) \tag{15}$$

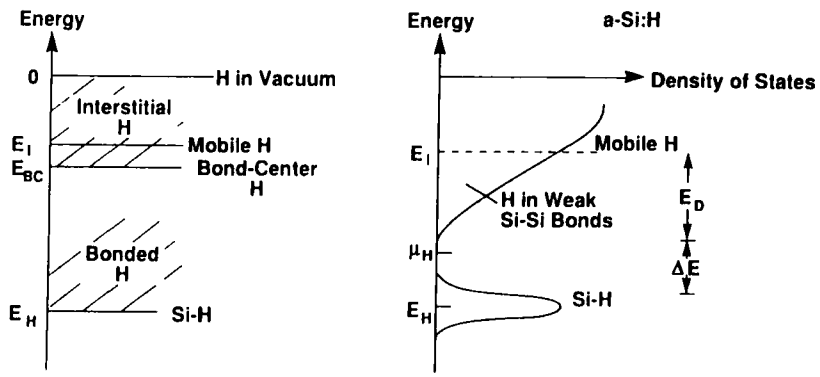

Figure 13. Illustration of the hydrogen energies in silicon. The left figure shows energy levels of interstitial and bonded H and the right figure is a simple model for a-Si:H that includes the disorder

where ν_0 is the attempt-to-escape frequency and E_t the transport edge (see Figure 13). Combining Equations (14) and (15) gives the time-dependent demarcation energy

$$E_t - E_D(t) = kT\ln(\nu_0 t) \tag{16}$$

States that are in thermodynamic equilibrium with transport levels at E_t are within the energy range E_t–$E_D(t)$; states that are deeper in energy are still frozen-in and represent therefore the non-equilibrated state. If we assume that the activation energy of τ represents the energy gap between transport levels and μ_H, then $E_{act} \approx E_t - \mu_H = kT\ln(\tau\nu_0)$. We can estimate ν_0 by use of the data shown in Figure 10, which gives ca. 10^{11}–$10^{12}\,s^{-1}$ for the phorphorus-doped layers and ca. $10^{14}\,s^{-1}$ for the boron-doped layers. The accuracy of the determination of ν_0 from the data in Figure 10 is, however, limited owing to the small investigated temperature regime, which makes the extrapolation of the data towards $T \to \infty$ speculative. Obviously for both phosphorus and boron doping the gap between E_t and μ_H is not affected by the dopants (boron or phosphorus) or the doping level but by the deposition temperature, which is increasing E_{act}. Whether E_t is shifted by deposition temperature variations, whether hydrogen is bonded differently or whether the HDOS is a function of T_s are open question that have to be solved before a generalized model of dopant metastability can be formulated.

Differences in kinetics between phosphorus- and boron-doped a-Si:H may reflect differences in local structure, as proposed by Liu and Spear.[10] In crystalline silicon, the hydrogen atom passivates boron by inserting between boron and a neighbouring silicon atom (see Figure 14), whereas hydrogen passivates phosphorus by locating in an antibonding site of an adjacent silicon atom, breaking the P–Si bond and removing the phosphorus donor level.[21–24] In both cases the measured passivation energies of ca. 1.1 eV are in reasonable agreement with theoretical predictions for phosphorus passivation (0.95–1.05 eV) and boron passivation (0.8–0.9 eV).[21] Instead of a single hydrogen atom, a two-H-atom complex H_2^* proposed by Chang and Chadi[24] is introduced to drive the passivation. The 10^3 times faster passivation in boron-doped a-Si:H has been attributed to a difference in the Fermi level (H_2^* dissociation is Fermi-level dependent); however, this cannot be confirmed by these experiments because for both samples $E_F - E_v \approx E_c - E_F$. The activation of dopants takes place by hydrogen emission. For the phosphorus–hydrogen complex, hydrogen is emitted out of the back bond in what is likely to be a single step process, whereas the emission and migration of hydrogen from the boron–hydrogen complex involves a rearrangement of at least three neighbouring atoms (C. G. Van de Walle, pers. comm.), which can give rise to the experimentally detected difference in dopant activation.

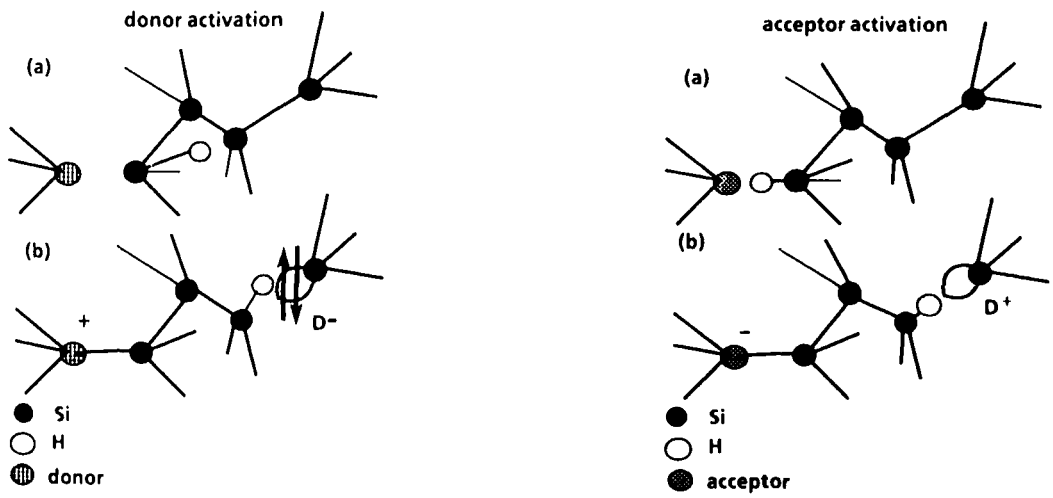

Figure 14. Schematic of donor and acceptor activation: (a) the initial, passive configuration; (b) the final, active configuration

Finally, we note that diffusion of charged hydrogen offers yet another mechanism that potentially relates the relaxation kinetics to the electronic state, because the concentration of charged species depends on the Fermi energy. Although it is difficult to determine which of these mechanisms dominates, the results indicate that interaction between the electronic and structural states play an important role in the relaxation kinetics.

Acknowledgements
The work was partially supported by the National Renewable Energy Laboratory, USA. C.E.N. is pleased to acknowledge partial support from the Alexander v. Humboldt Stiftung, Germany. The authors thank R. Thompson and C. C. Tsai for the preparation of high-quality a-Si:H.

REFERENCES

1. R. C. Chittick, R. C. Alexander and H. F. Sterling, 'The preparation and properties of amorphous silicon', *J. Electrochem. Soc.*, **116**, 77 (1969).
2. W. E. Spear and P. G. LeComber, 'Substitutional doping of amorphous silicon', *Solid State Commun.*, **17**, 1193 (1975).
3. W. B. Jackson and N. M. Amer, 'Direct measurement of gap state absorption in hydrogenated amorphous silicon by photothermal deflection spectroscopy', *Phys. Rev. B*, **25**, 5559 (1982).
4. C. R. Wronski, B. Abeles, T. Tiedje and G. D. Cody, 'Recombination centers in phosphorus doped hydrogenated amorphous silicon', *Solid State Commun.*, **44**, 1423 (1982).
5. R. A. Street, 'Doping and Fermi energy in amorphous silicon', *Phys. Rev. Lett.*, **49**, 1187 (1982).
6. R. A. Street, J. Kakalios and T. M. Hayes, 'Thermal equilibrium in doped amorphous silicon', *Phys. Rev. B*, **34**, 3030 (1986).
7. R. A. Street, J. Kakalios, C. C. Tsai and T. M. Hayes, 'Thermal-equilibrium processes in amorphous silicon', *Phys. Rev. B*, **35**, 1316 (1987).
8. R. A. Street, 'Hydrogen diffusion and electronic metastability in amorphous silicon', *Physica B*, **170**, 69 (1991).
9. G. Krötz, J. Wind, H. Stitzl, G. Müller, S. Kalbitzer and H. Mannsperger, 'Experimental tests of the autocompensation model of doping', *Philos. Mag. B*, **63**, 101 (1991).
10. E. Z. Liu and W. E. Spear, 'An investigation of the phosphorus doping mechanism in a-Si:H by sweep-out experiments', *Philos. Mag. B*, **64**, 245 (1991).
11. R. A. Street, 'Localized states in doped amorphous silicon', *J. Non-Cryst. Solids*, **77/78**, 1 (1985).
12. M. Stutzmann, D. K. Biegelsen and R. A. Street, 'Detailed investigation of doping in hydrogenated amorphous silicon and germanium', *Phys. Rev. B*, **35**, 5666 (1987).
13. R. A. Street, M. Hack and W. B. Jackson, 'Mechanisms of thermal equilibrium in doped amorphous silicon', *Phys. Rev. B*, **37**, 4209 (1988).
14. M. Hack and R. A. Street, 'Realistic modeling of the electronic properties of doped amorphous silicon', *Appl. Phys. Lett.*, **53**, 1083 (1988).
15. R. A. Street, 'Sweep-out measurements of the band-tail carriers in a-Si:H', *Philos. Mag. B*, **60**, 213 (1989).
16. J. Kakalios and R. A. Street, 'Thermal equilibrium effects in doped hydrogenated amorphous silicon', in *Amorphous Silicon Related Materials*, ed. by H. Fritzsche, p. 165. World Scientific Publishing, London, 1989.
17. K. Pierz, H. Mell and W. Fuhs, 'Defect density in doped a-Si:H films', in *Amorphous Silicon Technology 1990*, ed. by P. C. Tayler, M. J. Thompson, P. G. LeComber, Y. Hamakawa and A. Madan, *Mat. Res. Soc. Symp. Proc.*, **192**, 95 (1990).
18. J. Kakalios and W. B. Jackson, 'The hydrogen glass model', in *Amorphous Silicon Related Materials*, ed. by H. Fritzsche, p. 207. World Scientific Publishing, London, 1989.
19. K. Winer and W. B. Jackson, 'Universal dopant and defect equilibration kinetics in n-type a-Si:H', *Phys. Rev. B*, **40**, 12558 (1989).
20. N. M. Johnson, C. E. Nebel, P. V. Santos, W. B. Jackson, R. A. Street, K. S. Stevens and J. Walker, 'Stability of hydrogenated amorphous silicon deposited at high temperatures with a remote hydrogen plasma', *Appl. Phys. Lett.*, **59**, 1443 (1991).
21. W. B. Jackson, 'Microscopic mechanism for dopant activation in hydrogenated amorphous silicon', *Phys. Rev. B*, **41**, 12323 (1990).

22. W. B. Jackson, 'Role of hydrogen complexes in the metastability of hydrogenated amorphous silicon', *Phys. Rev. B*, **41**, 10257 (1990).
23. N. M. Johnson, 'Hydrogen in crystalline and amorphous silicon', *J. Non-Cryst. Solids*, **137/138**, 11 (1991).
24. K. J. Chang and D. J. Chadi, 'Theory of hydrogen passivation of shallow-level dopants in crystalline silicon', *Phys. Rev. Lett.*, **60**, 1422 (1988).
25. S. Taraskin, 'Thermalization in a system with a continuous spectrum of states', *J. Non-Cryst. Solids*, **137/138**, 25 (1991).